The adsorption of Direct Brown 1 dye using kaolinite and surfactant modified kaolinite

Mark Jeeva[1,*], Sivarama Krishna Lakkaboyana[2,3], Wan Zuhairi W.Y.[1]

[1]Geology Programme, Universiti Kebangsaan Malaysia, 43600 Bangi, Selangor, Malaysia
[2]Department for Management of Science and Technology Development,
Ton Duc Thang University, Ho Chi Minh City, Vietnam
[3]Faculty of Applied Sciences, Ton Duc Thang University, Ho Chi Minh City, Vietnam
*Corresponding author email address: mgva85@gmail.com

Abstract: This paper elucidates the removal of Direct Brown 1 (DB 1 1) dye from wastewater by using the natural kaolinite (NK) compared to Hexadecyltrimethylammonium bromide (HDTMA) modified kaolinite (HMK) as adsorbent materials at bench scale. The materials were characterized by X-Ray Diffraction (XRD) and FT-IR spectroscopy. The surface areas were determined using Sears' method. The test effects efficiency of natural and surfactant modified kaolinite in adsorption of DB 1 1 dye has been applied as a function of initial concentrations, pH, contact times and temperatures using the batch technique. Removal of dye from aqueous solution by HMK for the test effects showed a general increase of two to five times amount of DB 1 1 adsorbed compared to NK. The DB 1 1 adsorption was influenced by temperature with an increase of sorption (15 mg/g) for HMK compared to NK. The adsorption increased with temperature suggesting that the adsorption process was endothermic. The adsorption percentages of DB 1 for pH and contact time test effects showed 93 % and 82.7 % respectively for HMK compared to 6 % for NK. Adsorption percentages of DB 1 on equilibrium concentration effect resulted with 57.5 % for HMK compared to 6 % for NK. Intraparticle diffusion and mass driving force were found to be the reasons of increase rate of DB 1 adsorption onto HMK and NK. The temperature increase influenced the total energy of the adsorbate molecules to obtain a higher rate of adsorption. Pseudo-second-order of kinetics identifies rate limiting step as the chemical adsorption involving valent forces through sharing or interparticular diffusion between NK and HMK on DB 1. The adsorption patterns data correlated well with Langmuir ($R^2=0.93$) and Freundlich ($R^2=0.90$) isotherm models. From the comparison showed by increase in adsorption percentages, HMK was a better choice to be used as effective adsorbents for Direct Brown 1 (DB 1 1) dye compared to NK.

Keywords: Adsorption, Direct Brown 1 Dye, kaolinite, surfactant modified kaolinite

INTRODUCTION

In this modern world, day-by-day increases pollution in environment, due to rapid industrialization. These pollutants flow into the subsurface, occurs through waste disposals, industrial effluent outflow and chemical discharge through agricultural activities (Mohamed *et al.*, 2009). Application and usage of dyes in textile based industries is on the rise compared to other sectors to boost the economy of a country. Dyes entering waterways are less focused on since there are more reports of heavy metals, organic and inorganic compounds pollution. Dyes since their inception have diversified in terms of their types, functions and complexity. Synthetic dyes manufactured nowadays primarily are used in silk, wool, cotton related industries as they are durable, easily obtained and quick colour fastening. Tentatively, about 30 % of dyes used will be lost during the dying process, in which 10 – 15 % ends up in the surface and ground waterways. The problem occurs when coloured properties of dyes that can absorb and reflect light particles, making water less clear and displacing dissolved oxygen, degrading the aquatic ecosystem (Tang *et al.*, 2012). Dye effluents normally contain about 10 – 50 mg/L coloured concentration but in certain dyes, even a low level of 1 mg/L can be visibly detected (Mohan & Pittman, 2006). As a result

of this issue, dye treatments in waterways are rapidly gaining research potential in recent times (Chen *et al.*, 2013; Shu *et al.,* 2014). Water treatment technologies, including phytoextraction, reverse osmosis, electrodialysis, ion exchange and membrane filtration have also been developed to remove heavy metals and dyes from industrial wastewater. However, most of these methods have some disadvantages given the complicated processes involved: high cost and high energy consumption (Hong *et al.,* 2008; Krishna *et al.*, 2014). Adsorption process is found to be the most efficient method of effluent treatment because of the simple operative procedure, low cost and its directness. As such, determining new adsorption materials that are readily available and affordable are important for environmental protection (Wang *et al.,* 2008).

There are many materials used for contaminant adsorption currently in detailed research, mainly, activated carbon (Choi *et al.*, 2008; Mohan & Pittman, 2006), Nano Zero Valent Iron (NZVI) (Yaacob *et al.*, 2012; Wang *et al.*, 2013; Krishna *et al.*, 2017), zeolite (Li & Hong, 2009; Mahmoud *et al.,* 2014) and magnetite (Djomgoue *et al.*, 2012; Sivashankar *et al.*, 2014). Clay soil such as residual soil has good adsorption capacity and is also used as a clay liner at landfills to protect the groundwater from contaminants (Zuhairi *et al.*, 2008a). Kaolinite clay is chosen because of

its inexpensive and efficient adsorbent capability which has great potential in the application of heavy metal removal from wastewaters because of its abundance, chemical and mechanical stability, high adsorption capability, unique structural property, high Cationic Exchange Capacity (CEC) (15-75 meq/100 g) and high Specific Surface Area (SSA) (10-20 m²/g) (Adebowale *et al*., 2006). Sorptions of cationic surfactants, such as hexadecyltrimethylammonium (HDTMA) on clays were attributed to both cation exchange and hydrophobic bonding. As a result of hydrophobic bonding the sorbed surfactants form admicelle or bilayers which adsorb dyes. Dyes bearing a negative (anionic) charge, such as direct and acid dyes, are used because polyamides such as nylon and proteins such as wool, silk, and leather carry a positive (cationic) charge – especially during the dyeing process (Tang *et al*., 2012).

The main aim of this paper is to evaluate the adsorptive potency of natural kaolinite compared to Hexadecyltrimethylammonium bromide (HDTMA) modified kaolinite on an anionic trisazo dye. Natural kaolinite (NK) and HDTMA modified kaolinite (HMK) were used as effective adsorbents for Direct Brown 1 (DB 1) dye from an aqueous solution. The effects of experimental conditions on the removal efficiency, including adsorption time, pH, temperature, and initial DB 1 concentration were studied (Krishna *et al*., 2014). The possible adsorption mechanism of DB 1 onto HMK and HDTMA onto NK was proposed based on the information derived from HMK using FTIR and XRD spectrums (Jin *et al.,* 2013). Cationic Exchange Capacity (CEC), Specific Surface Area (SSA), kinetics of DB 1 adsorption using HMK and NK were also studied to explain the differences and effectiveness of surfactant modified kaolinite in dye adsorption.

MATERIALS AND METHODS
Materials
The natural kaolinite material was purchased from Kaolin (M) Sdn. Bhd. Company. All chemicals used in this study were of analytical reagent grade. Surfactant used is hexadecyltrimethylammonium (HDTMA) purchased from Merck Group. Dye used in this research is purchased from Sigma Aldrich (Unites States). The natural kaolinite (NK) was oven dried at 85 °C, screened through a 110-mesh sieve and then stored in a desiccator prior to use. Selected physical properties of the kaolinite are listed in Table 1.

Table 1: Some physical-chemical properties of kaolinite.

Parameters	NK	HMK
Size (µm)	50-150	50-150
XRD	Quartz, Kaolinite, Illite	Quartz, Kaolinite, Illite
CEC (meq/100g)	80	179
SSA (m²/g)	3.6	7.42
pH in distilled water	6	4.8

XRD-X-Ray Diffraction; CEC-Cationic Exchange Capacity; SSA-Specific Surface Area

Preparation of modified adsorbent and dye sorption solutions
Natural kaolinite (10 g) was added into a hexadecyltrimethylammonium (HDTMA) solution (50 mL) of known concentration and the mixture was maintained in a shaker incubator at 30 °C and 150 rpm for 24 h. The mixture was then centrifuged and the supernatant discarded. The precipitate was washed thoroughly with distilled water to remove any excess HDTMA. Adsorbent modification was prepared by adding to solutions containing 0.1, 0.25, 0.50, 0.75, 1.25, 2.0, 2.5 and 3.0 % of the HDTMA (w/w), thus making modified kaolinite samples of 0.05, 0.125, 0.25, 0.375, 0.625, 1.0, 1.25 and 1.5 g of HDTMA adsorbed on the kaolinite materials obtained after the multiplication of HDTMA's CEC value of 50. Stock solutions of DB 1 of different concentration were prepared by dissolving different amounts of the dye in distilled water. 0.1 mol/L HCl or 0.1 mol/L NaOH solution was used for the pH adjustment (Jin *et al.,* 2013). HMK values shown in Table 1 are stated after the optimal HDTMA modification of 0.25 g. All test effects analysis is done using the HMK with optimal HDTMA modification.

Chemical analysis and characterization
The FTIR spectra of NK and HMK were obtained using a Fourier transform infrared (FT-IR) spectrometer (Fourier-380FT-IR, America). The spectrum was recorded from 400 to 4000 cm-1 with a resolution of 2 cm-1 using a pressed KBr pellet. X-ray diffraction (XRD) spectroscopy was collected by the DIFFRAC.EVA software operating at 40 kV and 40 mA. The XRD pattern was recorded from 1.5 to 50 ° of 2θ with a 2θ scanning speed of 0.028 of per second. Morphology of kaolinite particles and average particle size were determined by Field Emission Scanning Electron Microscopy (FESEM) Zeiss Supra 55VP. The SSA was determined using the Sears' Method (1956) where the results were almost equivalent to (±0.5 to ±1.0 difference) B.E.T. method. SSA was conducted in the laboratory whereby, 0.5 g of each clay was acidified with 0.1 M HCl to a pH 3–3.5. The volume was made up to 50 mL with distilled water after addition of 10.0 g of NaCl. The titration was carried out with standard 0.1 M NaOH in a thermostatic bath at 298 ± 0.5 K to pH 4.0, and then to pH 9.0. The surface area was computed from the following equation:

$$S \ (m^2/g) = 32V - 25 \tag{1}$$

Where,
S = specific surface area of the adsorbent,
V= volume of NaOH required to raise the titrate pH from 4.0 to 9.0.

Adsorption experiment
The adsorption of DB 1 dye by NK and HMK was studied using batch experiments under the different conditions, including contact times (from 1 to 60 min),

pH (from 2.0 to 11.0), initial DB 1 concentrations (from 10 to 200 mg/L) and temperatures (25 to 75 °C). All the adsorption experiments were performed and recorded as results in triplicates. Batch experiments were performed in 50 mL capped plastic centrifuge tubes containing 50 mg/L DB 1 solutions (40 mL) and either NK or HMK (0.1 g) in a shaker incubator at the desired temperature and 200 rpm. After shaking for 1 hour, the suspensions were centrifuged at 3000 rpm for 10 minutes (Jin *et al.*, 2013; Uzum *et al.*, 2009). Dye Concentration remaining in the solution was determined by UV-VIS spectrophotometry. The amounts of DB 1 adsorbed by NK and HMK were calculated by difference using the following formula:

$$Qe = \frac{(Co-Ce)V}{m} \qquad (2)$$

Where:

Qe = the amount of dye adsorbed onto the natural kaolinite or modified kaolinite (mg/g)

Co = the initial concentration dye (mg/L)

Ce = the final value of dye concentration in the adsorbate (mg/L)

V = the volume of dye used (ml)

m = weight of natural kaolinite or modified kaolinite used (mg)

Adsorption equilibrium is usually described by an isotherm equation whose parameters express the surface properties and affinity of a solute on an adsorbent. Adsorption isotherms can be described by various models, of which the Langmuir and Freundlich models are the most common used (Unabonah *et al.*, 2008). The Langmuir model assumes that adsorption of molecules occurs on a surface of adsorbent at a fixed temperature, forming a monolayer without any interaction between molecules adsorbed on the surface. Freundlich's equation is used to describe adsorption of solute on a heterogeneous surface.

Effects of temperature, pH, point of zero charge (PZC), equilibrium concentration, adsorption kinetics and time

Adsorption experiments were carried out at various constant temperatures in ranges of 25-75 °C under the same adsorption isotherm experiments to explore the effect of temperature on adsorption of dye onto NK and HMK. The effect of pH on dye adsorption by NK and HMK was also examined in the initial pH ranges of 2 to 10 using Mettler-Toledo pH meter. The adsorbate was 40 ml of dye and solution pH was adjusted with 0.1 M NaOH and 0.1 M HCl. The time effect was assigned to be in the range between 1 and 60 minutes. The equilibrium concentration will be obtained by concentration value ranging from 1 mg/L to 200 mg/L in testing the adsorption extent of NK and HMK toward DB 1 dye. Adsorbent (0.1 g) was added in each adsorbate and reacted in the shaker for 24 hours at 25 °C.

This increase in adsorption with a rise in temperature can be explained on the basis of thermodynamic parameters

such as change in free energy ($\Delta G°$), enthalpy ($\Delta H°$) and entropy ($\Delta S°$) were calculated using the following equations:

$$(\Delta G°) = -RT \ln(K_c) \qquad (3)$$

$$\log Kc = \frac{\Delta S^o}{2.303R} - \frac{\Delta H^o}{2.303RT} \qquad (4)$$

where K_c is the equilibrium constant, R is the ideal gas constant (8.314 J/mol/K) and T is the adsorption temperature in Kelvin.

Adsorption equilibrium is usually described by an isotherm equation whose parameters express the surface properties and affinity of a solute on an adsorbent. Adsorption isotherms can be described by various models, of which the Langmuir and Freundlich models are the most common. The Langmuir model assumes that adsorption of molecules occurs on a surface of adsorbent at a fixed temperature, forming a monolayer without any interaction between molecules adsorbed on the surface. The model can be described by the following equation:

$$\frac{Ce}{Qe} = \frac{1}{KlQm} + \frac{1}{Qm} \times Ce \qquad (5)$$

where Q_e is the amount adsorbed (mg/g), C_e is the equilibrium concentration of the adsorbate (mg/L), and Q_m (mg/g) and K_l (L/mg) are Langmuir constants.

Freundlich's equation can also be used to describe adsorption of solute on a heterogeneous surface and is expressed as:

$$\log Qe = \log Kf + \frac{1}{n}\log C \qquad (6)$$

where Qe is the amount adsorbed (mg/g), Ce is the equilibrium concentration of the adsorbate (mg/L), and KF ($mg^{1-1/n} L^{1/n} g^{-1}$) and n (g/L) are the Freundlich constants, representing characteristics of the system, such as the adsorptive capacity and the adsorption intensity, respectively (Jin *et al.*, 2013).

The Point of Zero Charge (PZC) is an important characteristic of a solid phase immersed in a liquid medium and by knowing the PZC, conclusions on the sign of surface charge can be made, e.g. metal oxides are positively charged at pH < pH $_{PZC}$ and negatively charged at pH > pH $_{PZC}$, which give a better understanding of adsorption phenomena. Verification on the Point of Zero Charge was carried out using the technique adapted from Lazarevic *et al.* (2007). Initial pH values (pH$_i$) of 20 ml of KCl solutions (concentrations $10-2$ M) were adjusted in pH ranges of 2–11 using 0.01 M of HCl or NaOH. Then, 0.1 g of NK/HMK was added to each sample. Equilibration was carried out by shaking, in a water shaker and incubator at 200 rpm for 2 hour at 25 $\pm$ 1 °C. The dispersions were then filtered and the final pH of the solutions (pH$_f$) was determined. The point of zero charge was found from a plot of pH$_f$ vs. pH$_i$.

Due to the fast decrease in residual DB 1 concentration on a short time scale, implying strong adsorption interaction between the NK and HMK surfaces, a simple kinetic analysis

of adsorption, a pseudo-second-order equation, was used to fit experimental data in the present work as reported previously (Uzum, 2009; Jin *et al*., 2013). Its linear form can be given as (Sari, 2007):

$$\frac{t}{qt} = \frac{1}{(kqe2)} + \left(\frac{1}{qe}\right)t \tag{7}$$

where k is the rate constant of pseudo-second-order adsorption (gmg⁻¹ min⁻¹) and q_e and q_t are the amount (mg g⁻¹) of DB 1 dye adsorbed at equilibrium and time t, respectively. Rate parameters, k and qe, can be obtained directly from the intercept and slope of the plot of (t/q_t) against t. The equilibrium concentration (i.e., Ce) can be further calculated based on the mass balance concept, as the value of q_e has been obtained from the fitting of Equation (7). Also, half of the adsorption time, $t_{0.5}$, is the time required for the adsorbent to take up half as much DB 1 as it will have taken up at equilibrium (i.e., t =$t_{0.5}$ as q_t =q_e/2):

$$t0.5 = \frac{1}{kqe} \tag{8}$$

For adsorption kinetic studies 50 ml solution of DB 1 of 5.00×10 mol dm⁻³ concentration and 0.050 g of adsorbent were taken in a 100 ml Erlenmeyer flask. Keeping flask in a water bath and shaker, maintained at desired temperature, mixture was mechanically stirred. After a definite interval of time, the solution in the flask was filtered and filtrate of each was analyzed for the uptake of dye.

RESULTS AND DISCUSSIONS
Optimisation of HDTMA percentage on kaolinite

DB 1 adsorption on NK increased with increasing percentages of HDTMA, at 0.25 g, optimally 3.308 mg/g, compared to only 1.407 mg/g adsorbed on NK (Figure 1), suggesting that the increase in HDTMA content significantly enhanced the removal rate of DB 1 1 from solution. When HDTMA on K increased from 0.05 g to 0.1 g, DB 1 adsorbed on HMK increased from 1.407 mg/g to 2.321 mg/g, with a further increase to 3.309±0.001 mg/g (Table 2) when the HDTMA was 0.25 g. However, when HDTMA increased after 0.25 g onwards, the amount of DB 1 dye adsorbed recorded a slight decrease to 3.288

± 0.002 - 3.297 ± 0.002 mg/g (Table 2) implying that HDTMA on NK was excessively loaded and saturated when the amount was above 0.3 g. The adsorption capability can be improved using kaolinite modified with HDTMA. The CEC of NK was 268 meq/100 g when the HDTMA was 0.25 g, which was almost three times larger than NK (89 meq/100 g). Hence, 0.25 g of the HDTMA was considered as the optimal amount of HDTMA to be modified on the kaolinite.

Characterisation
FTIR analysis

Fourier Transform Infrared (FTIR) can be used to study surfactant surface configuration. Most band positions were not changed after HDTMA modification, suggesting that the basic crystal structure of NK and HMK remained unchanged. However, the bands corresponding to 2851 and 2920 cm⁻¹ from HMK were indicative of bilayer surfactant surface coverage on the kaolinite, symmetric and asymmetric stretching vibrations of C-C bonding in the alkyl chain. At a higher surface coverage, adsorbed HDTMA molecules resemble more with micelles than monomers as revealed by vibration band frequencies (Li & Gallus, 2005). The bands at 538 and 3621 cm⁻¹ are due to Al–O–Si stretching vibration and stretching vibration of -OH groups in kaolinite. The spectrum of HDTMA displays two split bands at 1482 and 1965 cm⁻¹ that are assigned to the aliphatic C–H stretching vibration (Vogel & Furniss, 1989). In Figure 2, HMK observed having a lower
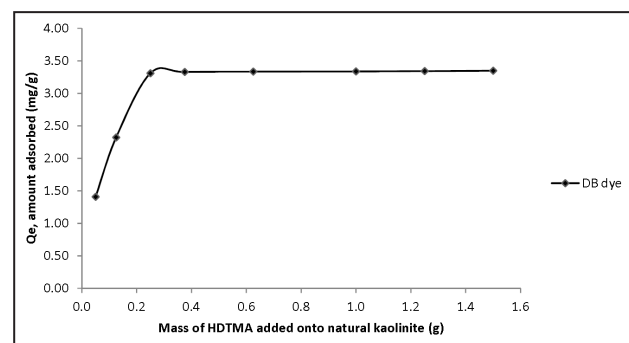

Figure 1: Relationship between amount of HDTMA and amount of DB adsorbed.

Table 2: Replication values and statistics of HDTMA amount and amount of DB adsorbed.

| Mass (g)	CTAB-Ben Qe1	CTAB-Ben Qe2	CTAB-Ben Qe3	Mean	Standard Deviation	Relative Standard Deviation	Standard Error
0.05	1.407	1.410	1.404	1.407	0.003	0.213	0.123
0.125	2.321	2.320	2.322	2.321	0.001	0.043	0.025
0.25	3.309	3.310	3.308	3.309	0.001	0.030	0.017
0.375	3.328	3.330	3.326	3.328	0.002	0.060	0.035
0.625	3.333	3.334	3.332	3.333	0.001	0.030	0.017
1	3.336	3.338	3.334	3.336	0.002	0.060	0.035
1.25	3.341	3.342	3.340	3.341	0.001	0.030	0.017
1.5	3.347	3.349	3.345	3.347	0.002	0.060	0.034
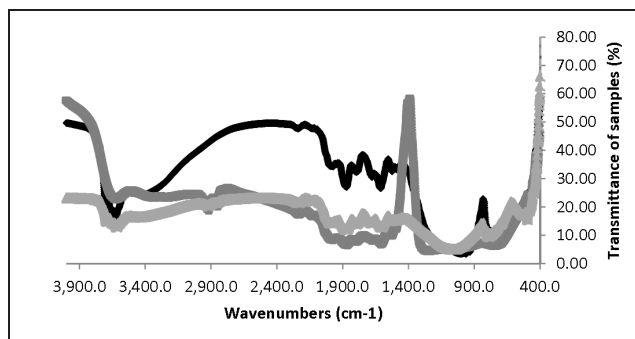
Figure 2: FTIR spectra of HDTMA, NK and HMK.

frequency vibration bands as an effect of surfactant loading denoting more ordered arrangement of adsorbed surfactant molecules. The stable HMK formed from HDTMA results in a complete surfactant admicelle configuration helps in the higher value of counterion adsorption resulting in higher adsorption affinity towards contaminants (Li & Gallus, 2007).

XRD and SEM analysis

The XRD patterns of NK, HMK and HMK adsorbed dye are given in Figure 3(a), which show the peaks of kaolinite and quartz. The XRD patterns showed no significant difference between NK and HMK, indicating HDTMA was not incorporated into the layers but covered the surface of NK after modification. The value in Figure 3(b) signifies peaks from DB 1 that differs from peaks of NK and HMK. However, the XRD pattern of DB 1 adsorbed on HMK is similar to that of only HMK, but intensity was decreased (79.7-239 a.u.), confirming that DB 1 ions were adsorbed on HMK by ion-exchange, where intensity increment happens when the cationic sites of HDTMA modified on the surface of NK (Jin *et al.*, 2013). SEM micrographs of NK and HMK are shown in Figure 4. The basal surface morphology of K was not smooth but showing very complex surface structure on the extensive (basal) plane with flaky interlayers and ragged, broken nano-sized edges which supported the adsorption of HDTMA. As a result HDTMA is evenly spread on the surface of NK thus reducing cluster formation of HDTMA (Ho & Zuhairi, 2015).

Specific Surface Area (SSA) analysis

The specific surface areas (SSA) of NK and HMK were measured following Sears' (1956) method in the laboratory. As HDTMA particles were dispersed onto the surface of NK, the reactivity was enhanced. The HMK SSA (7.42 m^2/g) is clearly larger than that of NK (3.60 m^2/g) showing that its reaction activity was much higher than NK due to more pronounced oxidation and aggregation. Therefore NK has only limited applications in remediation activities. In addition, while the surface of HMK was oxidized easily due to a higher specific surface area and stronger reactivity supported HMK was embedded in the double-layer structure of kaolin, which would decrease the oxidation of the HMK surface (Uzum *et al.*, 2009).
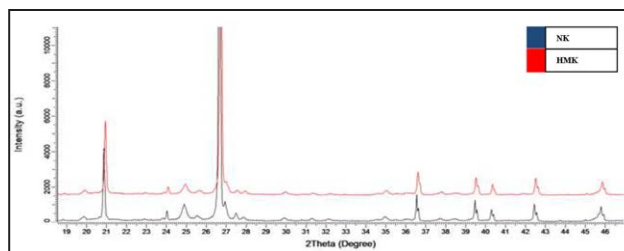

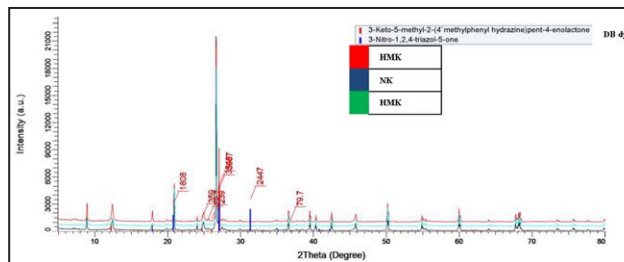**Figure 3 (a):** XRD pattern (Quartz) of NK and HMK.

Figure 3 (b): XRD pattern of DB dyes with values compared with NK (blue), HMK (red) and HMK adsorbed DB (green).
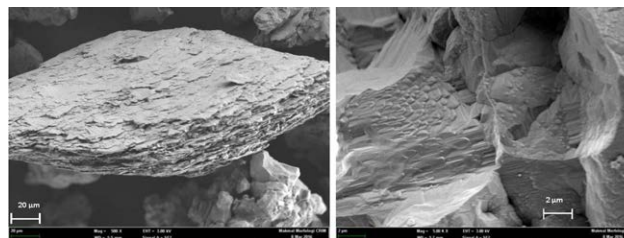

Figure 4: Scanning Electron Micrographs of NK (left) and HMK (right). NK has a flakey and jagged end-like structure alike all clayey materials. After modification HMK has dotted presence onto the surface of the flakes showing that successful mounting of HDTMA on NK.

Batch Test effects
Effects of temperature and time

Initial adsorption of DB 1 1 on HMK is rapid and DB 1 1 adsorption capacity increased with increasing contact time within the first 15 minutes, and remained almost constant suggests that the adsorption occurred on the exterior surface of the clay compared to the flat rate of slow adsorption of NK (3.16 to 3.28 ± 0.003). Therefore, a contact time range of 60 minutes was allowed for maximum adsorption as the remaining concentration of DB 1 after peaking is almost asymptotic to the time axis where the adsorption for HMK were in the range of 23.817 to 41.342 ± 0.003 units) (Table 3). The adsorption percentages of DB 1 showed an increase of 82.7 % for HMK compared to 6 % for NK (Figure 5). Following the increasing adsorption, diffusion into the internal clay particles controlled the adsorption rate as the exterior surface of the clay became saturated (Jin *et al.,* 2013). After the equilibrium time, the rate of DB 1 adsorption decreased and amount of DB 1 adsorbed remained the same. Temperature range from 25 ^{0}C to 75 ^{0}C where the results indicate an extensive increase of DB 1 adsorption on HMK, 36 ± 1 to 55 ± 1 mg/g (Table 4),

Table 3: Replication and statistics of contact times on the adsorption of DB on HMK and NK.

Time (min)	NK Qe1	NK Qe2	NK Qe3	Mean	Standard Deviation	Relative Standard Deviation	Standard Error
1	3.280	3.283	3.277	3.28	0.003	0.091	0.053
5	3.160	3.163	3.157	3.16	0.003	0.095	0.055
10	3.250	3.253	3.247	3.25	0.003	0.092	0.053
20	3.180	3.183	3.177	3.18	0.003	0.094	0.054
40	3.190	3.193	3.187	3.19	0.003	0.094	0.054
60	3.200	3.203	3.197	3.2	0.003	0.094	0.054
Time (min)	HMKQe1	HMKQe2	HMKQe3	Mean	Standard Deviation	Relative Standard Deviation	Standard Error
1	23.817	23.820	23.814	23.817	0.003	0.013	0.007
5	28.969	28.972	28.966	28.969	0.003	0.010	0.006
10	32.834	32.837	32.831	32.834	0.003	0.009	0.005
20	34.512	34.515	34.509	34.512	0.003	0.009	0.005
40	37.580	37.583	37.577	37.58	0.003	0.008	0.005
60	41.342	41.345	41.339	41.342	0.003	0.007	0.004

Table 4: Replication and statistics of temperature on the adsorption of DB on HMK and NK.

Temp (°C)	NKQe1	NKQe2	NKQe3	Mean	Standard Deviation	Relative Standard Deviation	Standard Error
25	25.381	25.384	25.378	25.381	0.003	0.012	0.007
35	24.354	24.357	24.351	24.354	0.003	0.012	0.007
45	26.219	26.222	26.216	26.219	0.003	0.011	0.007
55	26.624	26.627	26.621	26.624	0.003	0.011	0.007
65	26.708	26.711	26.705	26.708	0.003	0.011	0.006
75	26.976	26.979	26.973	26.976	0.003	0.011	0.006
Temp (°C)	HMKQe1	HMKQe2	HMKQe3	Mean	Standard Deviation	Relative Standard Deviation	Standard Error
25	36	37	35	36	1	2.778	1.604
35	36	37	35	36	1	2.778	1.604
45	48	49	47	48	1	2.083	1.203
55	52	53	51	52	1	1.923	1.110
65	54	55	53	54	1	1.852	1.069
75	55	56	54	55	1	1.818	1.050
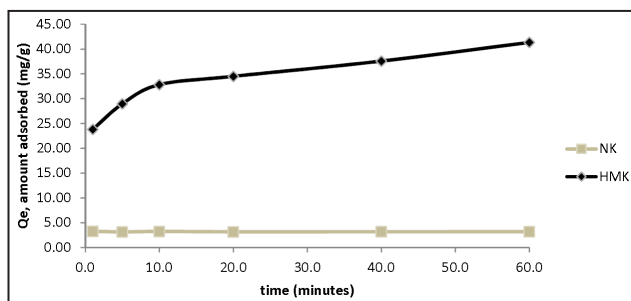
Figure 5: Effect of contact times on the adsorption of DB on HMK and NK.

compared to the flat readings of NK (Figure 6). As a result, adsorption percentage calculated an increase of 93 % of DB 1 1 adsorption on HMK compared to 6 % for NK. Increasing

adsorption capacity with increasing temperature shows that the adsorption of DB 1 is controlled by an endothermic reaction (Alkaram *et al.*, 2009).

The thermodynamic parameters, ΔH^o and ΔS^o were calculated from the slope and intercept of Van't Hoff plots of $\ln K_c$ versus $1/T$ (plots not shown). The thermodynamic parameters for the adsorption of NK and HMK on DB 1 1 are at various temperatures summarized in Table 9. The calculated ΔH^o values for NK and HMK are 13.78 and 29.85 kJ/mol, respectively. The positive value of ΔH^o indicates that the process is endothermic in nature. The negative values of ΔG^o showed the spontaneous adsorption of DB 11 on the adsorbents and the positive values of ΔS^o suggest that the increased randomness at the solid-solution interface during the adsorption of DB 1 1 in aqueous solution on NK and

HMK. The adsorbed solvent molecules which are displaced by the adsorbate species gain more translational entropy than ions lost by adsorbate thus allowing for prevalence of randomness in the system (Dizge *et al.*, 2008). In higher temperatures the total energy of the adsorbate molecules is increased thus, the adsorption of the adsorbate species is increased (Ho & Zuhairi, 2015).

Effect of pH

The effect of pH on DB 1 removal was investigated overnight in the pH range 2.0 – 11.0 at 25 °C with a DB 1 volume of 50 ml in 50 mg/L. The maximal adsorption capability of NK was 3.644 ± 0.002 mg/g compared with

Figure 6: Effect of temperature on the adsorption of DB on HMK and NK.

46.505 ± 0.003 mg/g (Table 5) for HMK at pH 6.0 (Figure 7). The pH significantly impacted more on the adsorption of DB 1 on HMK than on NK. As DB 1 was present in solution as an anionic species, NK could hardly adsorb any DB 1 at any pH. The adsorption capacity of DB 1 with HMK is increased with a general increase of pH values. Adsorption of clays at higher pH is higher and suggests that HDTMA modification covered the NK surfaces with positive charges and increased electrochemical interactions between anionic DB 1 dye molecules and the modified clay surfaces. Negatively charged species is readily adsorbed on positively charged clay surfaces due to stronger attractive forces at higher pH values. The high adsorption capacity is due to strong electrostatic interaction between the $N^+(CH_3)_3$ of HMK and $Na_2O_9S^-$ tail of DB 1 dye. Moreover, at lower pH more protons will be free, resulting in electrostatic repulsions, causing decrease in DB 1 adsorption. Similar findings have been reported by Alkaram *et al.* and Krishna *et al.* Adsorption of DB 1 on HMK increased in the pH range from 4.0 to 9.0, and then decreased significantly with increasing pH above 8. This was attributed to pH induced deprotonation of the functional groups in HDTMA (Jin *et al.*, 2013). HMK reached the equilibrium for DB 1 adsorption in pH 8 resulting in saturation overload that decreased the adsorption amount while in higher pH values. Following these results, pH was corrected as 8 in the adsorption of DB 1 on HMK and NK for all further test effect experiments.
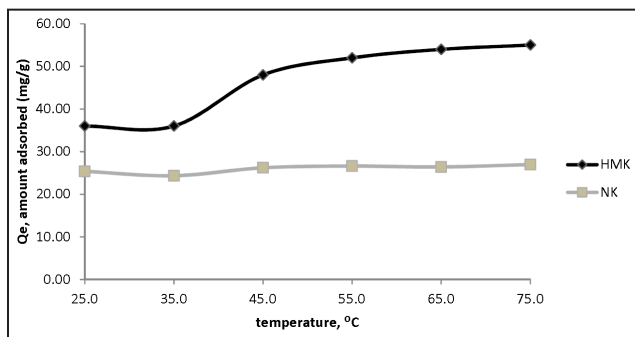
Table 5: Replication and statistics of pH on the adsorption of DB on HMK and NK.

| pH	NK Qe1	NK Qe2	NK Qe3	Mean	Standard Deviation	Relative Standard Deviation	Standard Error
2	3.738	3.740	3.736	3.738	0.002	0.054	0.031
3	3.646	3.648	3.644	3.646	0.002	0.055	0.032
4	3.511	3.513	3.509	3.511	0.002	0.057	0.033
5	3.516	3.520	3.512	3.516	0.004	0.114	0.066
6	3.459	3.458	3.460	3.459	0.001	0.029	0.017
7	3.416	3.418	3.414	3.416	0.002	0.059	0.034
8	3.375	3.377	3.373	3.375	0.002	0.059	0.034
9	3.327	3.329	3.325	3.327	0.002	0.060	0.035
10	3.287	3.289	3.285	3.287	0.002	0.061	0.035
11	3.241	3.243	3.239	3.241	0.002	0.062	0.036
pH	HMKQe1	HMKQe2	HMKQe3	Mean	Standard Deviation	Relative Standard Deviation	Standard Error
2	2.674	2.676	2.672	2.674	0.002	0.075	0.043
3	3.759	3.757	3.761	3.759	0.002	0.053	0.031
4	4.259	4.257	4.262	4.2593	0.003	0.059	0.034
5	45.451	45.454	45.448	45.451	0.003	0.007	0.004
6	46.505	46.508	46.502	46.505	0.003	0.006	0.004
7	45.827	45.830	45.824	45.827	0.003	0.007	0.004
8	42.972	42.975	42.969	42.972	0.003	0.007	0.004
9	39.216	39.219	39.213	39.216	0.003	0.008	0.004
10	6.216	6.219	6.213	6.216	0.003	0.048	0.028
11	4.505	4.508	4.502	4.505	0.003	0.067	0.038
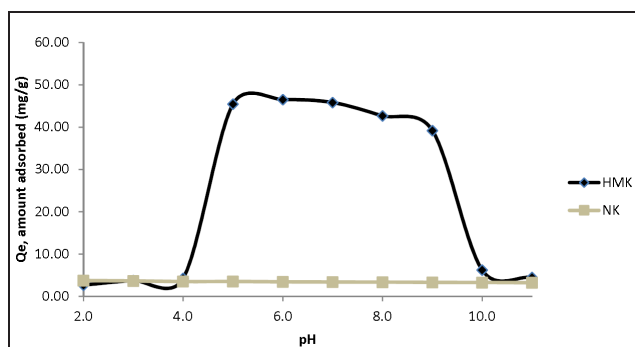
Figure 7: Effect of pH on the adsorption of DB on both HMK and NK.

The dependence of final pH (pH_f) vs. initial pH (pH_i) was plotted in Figure 8. The value of the Point of Zero Charge (PZC) was obtained as the pH value at which the curve plateau appeared between 10.1 ± 0.00 and 11.873 ± 0.025 (Table 6). At this pH value, a change in surface charge from positive to negative or vice versa has occurred. According to Figure 6, the plateau obtained at a pH value of 11 corresponded to the PZC of NK and HMK. Shift of the curves towards lower pH_{PZC} with increasing ionic strength for the KCl solutions may have attributed to the formation of $SO^-\cdot K^+$ surface complexes due to columbic interactions (Tang *et al.*, 2012).

Effect of equilibrium concentration and adsorption isotherm

Equilibrium DB 1 concentrations were found to be in the range of 10-200 mg/L for adsorption on HMK and NK at pH 8 and 25 ^{O}C for 24 hour interaction. As shown in Figure 9, increase in equilibrium DB 1 concentration
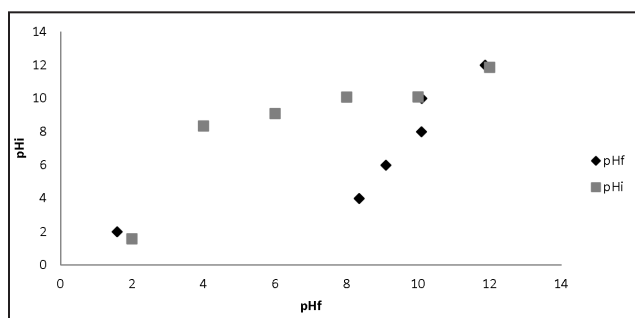
results in an increase in adsorption of DB 1 on HMK. When concentration of DB 1 increased from 10 to 200 mg/L, the adsorption of DB 1 increased from 5.748 ± 0.002 to 89.932 ± 0.002 mg/g (Table 7). The maximal equilibrium point in adsorptive capacity of DB 1 on HMK and NK was 89.932 ± 0.002 and 13.139 ± 0.003 mg/g, respectively. Thus, the adsorptive percentage of HMK on DB 1 increased about 57.5 % compared to 12 % of NK. HMK has more adsorption active sites available for further adsorption explaining the five times percentage increase compared to NK as it saturated and plateau rapidly.

As listed in Table 8, linear plots of Ce/Qe versus Ce were used to determine Q_0 and K_L. The Langmuir adsorption Q_0 of HMK was high (22.8 mg/g) compared to the Q_0 of K (0.5 mg/g), and the Langmuir equilibrium constant K_L, was 0.0049 and 0.011 L/mg for HMK and K, respectively. Comparison of the correlation coefficients showed that the Langmuir equation ($R^2 = 0.9295$) fit the adsorption of DB 1 on HMK better than the Freundlich equation ($R^2 = 0.9007$). Jaynes & Boyd (1991), proposed that the adsorption conforms to the Langmuir and Freundlich models when the value of correlation coefficient (R^2) is greater than 0.89. As a result, the indications are that both HMK and NK were suitable adsorbents for the removal of DB 1 from aqueous solution. From linear plots of the Freundlich isotherm, K_F and n were found to be 0.28 and 0.01, respectively for HMK and 1.5 and 1.87 g/L for K, respectively. If a value for n is equal to unity, this implies that adsorption process is chemical, but a value for n is above to unity, adsorption is favourable a physical process. Since the Freundlich constant n was greater than 1, this indicated that adsorption was favourable physical process
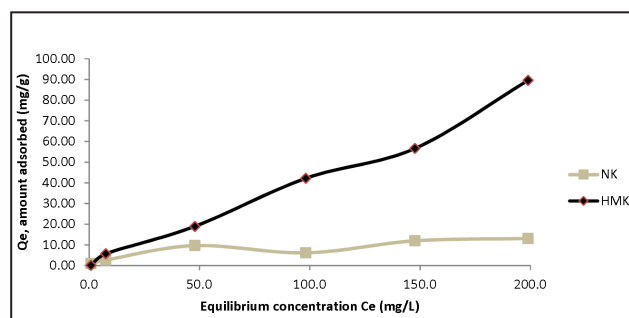

Figure 8: Dependence of pHf on pHi during equilibrium of 0.1g of NK and HMK with KCl to determine PZC.

Figure 9: Effect of equilibrium concentration (C_e) on the adsorption of DB on NK and HMK.

Table 6: Replication and statistics of PZC on the adsorption of DB on HMK and NK.

pHi	pH_f1	pH_f2	pH_f3	Mean	Standard Deviation	Relative Standard Deviation	Standard Error
2	1.58	1.6	1.59	1.59	0.01	0.629	0.363
4	8.35	8.36	8.34	8.35	0.01	0.120	0.069
6	9.1	9.2	9	9.1	0.1	1.099	0.634
8	10.09	10.11	10.07	10.09	0.02	0.198	0.114
10	10.1	10.1	10.1	10.1	0.000	0.000	0.000
12	11.87	11.9	11.85	11.873	0.025	0.212	0.122

Table 7: Replication and statistics of equilibrium concentration (C_e) on the adsorption of DB on HMK and NK.

Ce NK	Qe1 NK	Qe2 NK	Qe3 NK	Mean	Standard Deviation	Relative Standard Deviation	Standard Error
0.865	0.988	0.991	0.985	0.9879	0.003	0.304	0.175
7.575	2.655	2.658	2.652	2.6545	0.003	0.113	0.065
47.897	9.685	9.688	9.682	9.6848	0.003	0.031	0.018
98.220	10.170	10.173	10.167	10.17	0.003	0.029	0.017
147.633	11.988	11.991	11.985	11.988	0.003	0.025	0.014
198.953	13.139	13.142	13.136	13.139	0.003	0.023	0.013
Ce HMK	**Qe1 HMK**	**Qe2 HMK**	**Qe3 HMK**	**Mean**	**Standard Deviation**	**Relative Standard Deviation**	**Standard Error**
0.865	0.135	0.137	0.133	0.135	0.002	1.481	0.855
7.575	5.748	5.750	5.746	5.748	0.002	0.035	0.020
47.897	18.974	18.976	18.972	18.974	0.002	0.011	0.006
98.220	42.199	42.201	42.197	42.199	0.002	0.005	0.003
147.633	56.628	56.630	56.626	56.628	0.002	0.004	0.002
198.953	89.932	89.934	89.930	89.932	0.002	0.002	0.001

Table 8: Isothermal equation parameters of the adsorption of DB on HMK and NK.

Parameters	Langmuir			Freundlich		
	Qe (mg/g)	K_L (L/g)	R^2	K_F (mg$^{1-1/n}$L$^{1/n}$g^{-1})	N (g/L)	R^2
NK	0.5	0.011	0.8574	0.01	1.5	0.8481
HMK	22.8	0.0049	0.9295	0.28	1.87	0.9007

under the studied conditions. The obtained n value was assigned to the heterogeneous nature of adsorbent surface with an exponential distribution of the adsorption energy sites (Granados-Correa & Becerril, 2009). The Langmuir and Freundlich constants both suggested that HMK have a higher adsorptive capacity than that of NK for removing DB 1 from aqueous solution. The applicability of the two isotherm models to the all investigated systems implies that both monolayer adsorption (i.e., only a limited number of surface sites are adsorbing sites) and heterogeneous surface conditions exist under the experimental conditions studied. Organically modified clays are much more efficient adsorbents of DB 1 than the unmodified NK. Unmodified NK has an adsorption complication due to the limited surface area (short-chained carbon, (C < 10)) whereas partitioning complication is the organic partitioning using the long-chained carbon (C > 10), modifiers of HMK provides no limitation for adsorption (Alkaram *et al*., 2009).

Effects of adsorption kinetics

It is clear that the removals of the dyes were dependent on the concentration of the dyes. The rate of adsorption decreased with time until it gradually approached a plateau due to the continuous decrease in the concentration driving force. Moreover, the initial rate of adsorption was greater for higher initial dye concentration since the resistance to the dye uptake decreased as the mass transfer driving force increased. Table 10 shows the pseudo-second-order

Table 9: Thermodynamic parameters for the adsorption of DB on HMK and NK.

Material	Temperature (K)	-ΔG (Kj/mol)	ΔH (Kj/mol)	ΔS (Kj/mol)	r^2
NK	298	4.08			
	308	4.24			
	318	4.89	13.78	0.079	0.88
	328	4.93			
	338	5.23			
	348	5.47			
HMK	298	8.45			
	308	8.87			
	318	9.28	29.85	0.166	0.95
	328	9.78			
	338	10.54			
	348	10.87			

parameters for adsorption of DB 1 onto NK and HMK and the rate limiting step of both materials at various equilibrium concentrations. From Equation (8), it was found that the intraparticle diffusion coefficients, k, and half of the adsorption time, $t^{0.5}$, increased with the increasing of the equilibrium dye concentration (Dizge *et al*., 2008). The rate limiting step implies to the occurrence of chemical

Table 10: Pseudo-second-order parameters for adsorption of DB onto NK and HMK at various initial concentrations.

Initial concentrations (mol dm^{-3})	k (g mg^{-1}min^{-1})	q_e (mg g^{-1})	R^2	Ce (mol dm^{-3})	$t_{0.5}$ (min)	Concentration of NK and HMK	Rate Limiting Step
1	1.8	9.01	0.96	0.08	1.9	1000	1800
10	1.1	18.9	0.97	0.53	2.1	1000	11000
50	0.5	57.8	0.96	10.7	2.7	1000	25000
100	0.07	92.4	0.98	38.7	2.9	1000	7000
150	0.005	120.8	0.98	54.1	3.6	1000	750
200	0.002	170.6	0.96	87.8	3.9	1000	400

adsorption involving valence forces through sharing or interparticular diffusion between NK and HMK on DB 1 (Sivashankar *et al.*, 2014).

CONCLUSIONS

The modification of natural kaolinite with HDTMA increases both the specific surface area and CEC significantly, and as a result HMK can be used to remove DB 1 from aqueous solution. The amount of DB 1 adsorbed on HMK compared to NK was 2 to 3 times higher in temperature tests, 5 times higher in pH changes from 4.0 to 9.0, 6 to 8 times higher in time effects and 9 times higher in maximum initial concentration adsorption. FTIR and XRD analysis shows that HDTMA adsorb on the surface of the kaolinite are responsible for the DB 1 adsorption. The Langmuir equation ($R^2 = 0.93$) is the best fit for the adsorption of DB 1 on HMK shows that the adsorption of DB 1 occurred on the surface of HMK. A rapid increase in DB 1 adsorption by HMK especially showed a higher rate in temperature dependence (29.85 kJ/mol) and resulted in a pseudo-second-order reaction. In addition, isotherms and thermodynamic parameters indicated the adsorption was an endothermic process occurring on a heterogeneous surface, which required some external energy input. These results show that little amount of surfactant modified kaolinite is very efficient and cost effective in removing DB 1 dye from the water systems.

ACKNOWLEDGEMENTS

REFERENCES

Adebowale, K.O., Unuabonah, I.E. & Olu-Owolabi, B.I., 2006. The effect of some operating variables on the adsorption of lead and. cadmium ions on kaolinite clay. Journal of Hazardous Materials, 134 (1-3), 130-9.

Alkaram, U.F., Mukhlis, A.A. & Al-Dujaili, A.H., 2009. The removal of phenol from aqueous solutions by adsorption using surfactant-modified bentonite and kaolinite. Journal of Hazardous Materials, 169, 324–332.

Chen, Z., Wang, T., Jin, X., Chen, Z., Megharaj, M. & Naidu, R., 2013. Multifunctional kaolinite-supported nanoscale zero-valent iron used for the adsorption and degradation of crystal violet in aqueous solution. Journal of Colloid and Interface Science, 398, 59–66.

Choi, H.-D., Shin, M.-C., Kim, D.-H., Jeon, C.-S. & Baek, K., 2008. Removal characteristics of reactive black 5 using surfactant-modified activated carbon. Desalination, 223(1-3), 290–298.

Dizge, N., Aydiner, C., Demirbas, E., Kobya, M., & Kara, S., 2008. Adsorption of reactive dyes from aqueous solutions by fly ash: kinetic and equilibrium studies. Journal of Hazardous Materials, 150(3), 737–46.

Djomgoue, P., Siewe, M., Djoufac, E., Kenfack, P. & Njopwouo, D., 2012. Surface modification of Cameroonian magnetite rich clay with Eriochrome Black T. Application for adsorption of nickel in aqueous solution. Applied Surface Science, 258(19), 7470–7479. doi:10.1016/j.apsusc.2012.04.065.

Granados-Correa, J.F. & Becerril, J., 2009. Chromium (VI) adsorption on boehmite. Applied Clay Science, 35, 250–257.

Ho K. H. & W. Y. Wan Zuhairi, 2015. Synthesis and characterization of marine clay- supported nano zero valent iron. American Journal of Environmental Sciences, 11(2), 115-124.

Hong, H., Jiang, W., Zhang, X., Tie, L. & Li, Z., 2008. Adsorption of Cr(VI) on STAC modified rectorite. Appl. Clay Sci., 42, 292.

Jaynes, W.F. & Boyd, S.A., 1991. Hydrrophobicity of siloxane surfaces in smectites as revealed by aromatic hydrocarbon adsorption from water. Clays and Clay Minerals, 39 (4), 428-436.

Jin, X., Jiang, M., Duc, J. & Chen, Z., 2013. Removal of Cr(VI) from aqueous solution by surfactant-modified kaolinite. Journal of Industrial and Engineering Chemistry, 20(5), 3025-3032

Krishna, L.S., Soontarapa, K., Yuzir, A., Kumar, V.A. & Zuhairi, W.Y.W., 2017. Kaolin-nano scale zero-valent iron composite (K-nZVI): synthesis, characterization and application for heavy metal removal. Desalination and Water Treatment, 100, 168-177.

Krishna, L.S., Sreenath Reddy, A., Wan Zuhairi, W. Y., Taha, M. R. & Varada Reddy, A., 2014. Indian jujube seed powder as an eco-friendly and a low-cost biosorbent for removal of acid blue 25 from aqueous solution. Scientific World Journal, 18, 40-58.

Lazarevic, S., Jankovic-Castvan, I., Jovanovic, D., Milonjic, S., Janackovic, D. & Petrovic, R., 2007. Adsorption of Pb^{2+} Cd^{2+} and Sr^{2+} ions onto natural and acid-activated Sepiolites. Appl. Clay Sci., 37, 47–57.

Li, Z. & Gallus, L., 2005. Surface configuration of sorbed hexadecyl-trimethylammonium on kaolinite as indicated by surfactant and counterion sorption, cation desorption, and FTIR. Colloids Surf., A Physicochem. Eng. Asp., 264, 61–67.

Li, Z. & Gallus, L., 2007. Adsorption of dodecyl trimethylammonium and hexadecyl trimethylammonium onto kaolinite - Competitive adsorption and chain length effect. J. Hazard. Mater., 162, 1178.

Li, Z. & Hong, H., 2009. Retardation of chromate through packed columns of surfactant-modified zeolite. Journal of Hazardous

Materials, 162(2-3), 1487–93.

Mahmoud, E. & Lobo, R.F., 2014. Recent advances in zeolite science based on advance characterization techniques. Microporous and Mesoporous Materials, 189, 97–106.

Mohamed, A.F., Wan Yaacob, W. Z., Taha, M. R. & Samsudin, A.R., 2009. Groundwater and soil vulnerability in the Langat basin Malaysia. European Journal of Scientific Research, 27(4), 628-635.

Mohan, D. & C.U. Pittman Jr., 2006. Activated carbons and low cost adsorbents for remediation of tri- and hexavalent chromium from water. J. Hazard. Mater., B137, 762.

Reddy, M.C.S, Sivaramakrishna, L. & Varada Reddy, A., 2012. The use of an agricultural waste material, Jujuba seeds for the removal of anionic dye (Congo red) from aqueous medium. Journal of Hazardous Materials, 203-204, 118-127.

Sari, A., Tuzen, M., Citak, D. & Soylak, M., 2007. Equilibrium, kinetic and thermodynamic studies of adsorption of Pb(II) from aqueous solution onto Turkish kaolinite clay. Journal of Hazardous Materials, 149(2), 283-291.

Sears, G., 1956. Determination of specific surface area of colloidal silica by titration with sodium hydroxide. Anal. Chem., 28, 1981–1983.

Shu, Z., Li, T., Zhou, J., Chen, Y., Yu, D. & Wang, Y., 2014. Template-free preparation of mesoporous silica and alumina from natural kaolinite and their application in methylene blue adsorption. Applied Clay Science, 102, 33–40.

Sivashankar, R., Sathya, A. B., Vasantharaj, K. & Sivasubramanian, V., 2014. Magnetic composite an environmental super adsorbent for dye sequestration – A review. Environmental Nanotechnology, Monitoring & Management, 1(2), 36–49.

Tang, J., Yang, Z.F. & Yi, Y.J., 2012. Enhanced Adsorption of Methyl Orange by Vermiculite Modified by Cetyltrimethylammonium Bromide (CTMAB). Procedia Environmental Sciences, 13, 2179 – 2187.

Unuabonah, E.I., Adebowale, K.O., Olu-Owolabi B.I., Yang L.Z., Kong & L.X., 2008. Adsorption of Pb (II) and Cd (II) from aqueous solutions onto sodium tetraborate-modified Kaolinite clay: Equilibrium and thermodynamic studies. Hydrometallurgy, 93(1–2), 1-9.

Üzüm, Ç., Shahwan, T., Eroğlu, A.E., Hallam, K.R., Scott T.B. & I. Lieberwirth, 2009. Synthesis and characterization of kaolinite-supported zero-valent iron nanoparticles and their application for the removal of aqueous Cu^{2+} and Co^{2+} ions. Applied Clay Science, 43, 172–181.

Vogel, A.I. & Furniss, B.S., 1989. Vogel's textbook of practical organic chemistry. Longman, 1417-1421.

Wang, T., Su, J., Jin, X., Chen, Z., Megharaj, M. & Naidu, R., 2013. Functional clay supported bimetallic nZVI/Pd nanoparticles used for removal of methyl orange from aqueous solution. Journal of Hazardous Materials, 262, 819–825.

Wang, Y., Lan, Y. & Hu. Y., 2008. Surfactant assisted bioremediation of hexavalent chromium from contaminated water. Miner. Eng., 21, 913.

Yaacob, W.Z.W., Kamaruzaman, N. & Samsudin, A. R., 2012. Development of nano- zero valent iron for the remediation of contaminated water. Chemical Engineering Transactions, 28, 25-30.

Zuhairi, W.Y.W., Samsudin, A.R. & Kong, T.B., 2008a. The sorption distribution coefficient of lead and copper on the selected soil samples from Selangor. Bulletin of the Geological Society of Malaysia, 54, 21-25.